J Neurogastroenterol Motil, Vol. 29 No. 2 April, 2023
pISSN: 2093-0879 eISSN: 2093-0887
https://doi.org/10.5056/jnm22078
Journal of Neurogastroenterology and Motility

Original Article

Transcriptome and Proteome Profiling of Primary Human Gastric Interstitial Cells of Cajal Predicts Pacemaker Networks

Daphne Foong,[1] Meena Mikhael,[1] Jerry Zhou,[1] Ali Zarrouk,[2] Xiaodong Liu,[3,4,5] Jan Schröder,[3,4,5] Jose M Polo,[3,4,5] Vincent Ho,[1,2] and Michael D O'Connor[1]*

[1]Regenerative Medicine Laboratory, School of Medicine, Western Sydney University, Campbelltown, NSW, Australia; [2]South West Surgery, Campbelltown Private Hospital, Campbelltown, NSW, Australia; [3]Department of Anatomy and Developmental Biology, Monash University, Clayton, VIC, Australia; [4]Development and Stem Cells Program, Monash Biomedicine Discovery Institute, Clayton, VIC, Australia; and [5]Australian Regenerative Medicine Institute, Monash University, Clayton, VIC, Australia

Background/Aims
Interstitial cells of Cajal (ICC) are specialized gastrointestinal (GI) pacemaker cells required for normal GI motility. Dysfunctions in ICC have been reported in patients with GI motility disorders, such as gastroparesis, who exhibit debilitating symptoms and greatly reduced quality of life. While the proteins, calcium-activated chloride channel anoctamin-1 (ANO1) and the receptor tyrosine kinase (KIT), are known to be expressed by human ICC, relatively little is known about the broad molecular circuitry underpinning human ICC functions. The present study therefore investigates the transcriptome and proteome of ANO1-expressing, $KIT^{low}/CD45^{-}/CD11B^{-}$ ICC obtained from primary human gastric tissue.

Methods
Excess human gastric tissue resections were obtained from sleeve gastrectomy patients. ICC were purified using fluorescence-activated cell sorting (FACSorting). Then, ICC were characterized by using immunofluorescence, real-time polymerase chain reaction, RNA-sequencing and mass spectrometry.

Results
Compared to unsorted cells, real-time polymerase chain reaction showed the $KIT^{low}/CD45^{-}/CD11B^{-}$ ICC had: a 9-fold ($P < 0.05$) increase in *ANO1* expression; unchanged KIT expression; and reduced expression for genes associated with hematopoietic cells (*CD68*, > 10-fold, $P < 0.001$) and smooth muscle cells (*DES*, > 4-fold, $P < 0.05$). RNA-sequencing and gene ontology analyses of the $KIT^{low}/CD45^{-}/CD11B^{-}$ cells revealed a transcriptional profile consistent with ICC function. Similarly, mass spectrometry analyses of the $KIT^{low}/CD45^{-}/CD11B^{-}$ cells presented a proteomic profile consistent with ICC activities. STRING-based protein interaction analyses using the RNA-sequencing and proteomic datasets predicted protein networks consistent with ICC-associated pacemaker activity and ion transport.

Conclusion
These new and complementary datasets provide a valuable molecular framework for further understanding how ICC pacemaker activity regulates smooth muscle contraction in both normal GI tissue and GI motility disorders.
(J Neurogastroenterol Motil 2023;29:238-249)

Key Words
Bioinformatics; Gastrointestinal motility; Interstitial cells of Cajal; Proteome transcriptome

Received: June 15, 2022 Revised: December 11, 2022 Accepted: December 19, 2022

*Correspondence: Michael D O'Connor, PhD
Regenerative Medicine Laboratory, Western Sydney University, Locked Bag 1797, Penrith NSW 2751, Australia
Tel: +61-2-4620-3902, E-mail: m.oconnor@westernsydney.edu.au

Introduction

Interstitial cells of Cajal (ICC) are specialized gastrointestinal (GI) pacemaker cells required for normal GI motility. ICC generate and propagate slow wave activity through to smooth muscle cells, and also mediate neurotransmission from enteric neurons.[1] Abnormalities in ICC numbers and structure have been implicated in several GI motility disorders, such as gastroparesis.[2,3]

The receptor tyrosine kinase KIT,[4-6] and the calcium-activated chloride channel anoctamin-1 (ANO1),[7] are known to be expressed by ICC in the GI tract. ANO1 is involved in initiating and propagating slow wave activity.[7,8] ANO1 is also considered to be a more specific marker of GI ICC, as KIT is expressed by other cell types in the gut such as macrophages and mast cells (MCs).[9,10] However, effective anti-ANO1 antibodies for cell purification are yet to be commercially available. Consequently, anti-KIT antibodies have been routinely used for ICC purification via fluorescence-activated cell-sorting (FACSorting), particularly for isolation of mouse ICC.[10-12]

Molecular characterization studies of primary ICC isolated using anti-KIT antibodies have largely been based on mouse GI tissues.[13] Transcriptome profiling of FACSorted Kit$^+$ primary mouse ICC, using microarray and RNA-sequencing (RNA-seq), have provided insights into the cellular and biological identity of ICC.[11,14] Due to difficulties accessing human GI tissue for research, only 2 (microarray-based[15] and single-cell RNA-seq-based[16]) transcriptomic profiling study of FACSorted primary human gastric ICC have been published, with no bulk RNA-seq or proteomic profiles reported.

For the present study, bulk populations of human gastric ICC were captured from excess sleeve gastrectomy tissues using antibodies against KIT, CD45, and CD11B (ie, KIT^{low}/CD45$^-$/CD11B$^-$ cells). RNA-seq and shotgun proteomics-based mass spectrometry were then used to generate and compare transcriptome and proteome profiles of the purified human ICC. The bulk RNA-seq data were consistent with previously acquired single-cell RNA-seq (scRNA-seq) data similarly obtained from primary human gastric KIT^{low}/CD45$^-$/CD11B$^-$ cells.[16] Further analyses of the bulk RNA-seq and mass spectrometry datasets revealed a large overlap between the genes and proteins expressed by the human gastric KIT^{low}/CD45$^-$/CD11B$^-$ ICC—both in terms of the individual genes and proteins expressed, as well as the predicted protein interaction networks associated with ICC-related activities (such as regulation of muscle contraction).

Materials and Methods

Consent for Use of Human Gastric Tissue

The use of human gastric tissues and associated experimental procedures were approved by the Western Sydney University Human Research Ethics Committee (#H11683), and were performed in accordance with the Declaration of Helsinki (version 2013). Human gastric resections were collected from patients undergoing laparoscopic sleeve gastrectomy at Campbelltown Private Hospital (Sydney, Australia). All tissues were collected after obtaining informed and written consent.

Immunofluorescence

Human gastric tissue was dissected to remove the mucosa, submucosa, and associated fat, leaving only the smooth muscle. Gastric muscle pieces were embedded in Tissue-Tek O.C.T. compound (ProSciTech, Townsville, Australia), frozen in liquid nitrogen and stored at −80℃. Samples were sectioned at 20 μm using a Leica CM1950 cryostat (Leica Biosystems, Sydney, Australia) onto poly-L-lysine-coated slides (Sigma, Sydney, Australia). Sections were equilibrated at room temperature (≥ 2 hours), fixed in acetone (4℃, 10 minutes; Chem-Supply, Adelaide, Australia), rinsed with phosphate-buffered saline (PBS; 2 × 5 minutes; Thermo Fisher Scientific, Sydney, Australia), blocked in 1% bovine serum albumin (BSA; room temperature, 1 hour; Sigma)/PBS and incubated with primary antibody (4℃, overnight) in 0.3% Triton X (Sigma) with 1% BSA/PBS. Sections were then washed with PBS (3 × 5 minutes), incubated with secondary antibody (room temperature, 1 hour) in 0.3% Triton X-100/1% BSA/PBS, washed again with PBS (3 × 10 minutes), and treated with ProLong Gold Antifade Mountant containing DAPI (Thermo Fisher Scientific). Images

were captured using a Zeiss Axio Imager M2 microscope (Sydney, Australia) with MBF Biosciences StereoInvestigator software (2019; Williston, ND, USA). Primary antibodies used were: anti-ANO1 rabbit IgG polyclonal (Abcam, Melbourne, Australia) and anti-KIT mouse IgG1 monoclonal (Thermo Fisher Scientific). Secondary antibodies used were: Alexa Fluor 488 goat anti-rabbit IgG, and Alexa Fluor 594 goat anti-mouse IgG (Thermo Fisher Scientific). Controls were prepared by omitting primary antibodies.

Interstitial Cells of Cajal Purification via Fluorescence-activated Cell-sorting

Human gastric smooth muscle tissue resections were manually minced into ~1 mm^3 pieces using scissors and submerged in Dulbecco's Modified Eagle Medium containing 0.2% collagenase type IV (Thermo Fisher Scientific) and 0.02% DNase I (Sigma) for 1 hour at 37℃ in a 5% CO_2 incubator. Cell suspensions were sequentially filtered through stainless steel mesh strainers followed by 100 μm and 40 μm cell strainers (Miltenyi Biotec, Sydney, Australia; and Sigma), prior to red blood cell lysis using ACK Lysing Buffer (1 mL, room temperature, 30-60 seconds; Thermo Fisher Scientific). Cell suspensions were stained (4℃, 20 minutes) with Human Fc Receptor Blocking Reagent (20 μL/10^7 cells; Miltenyi Biotec) and primary antibodies: anti-KIT-APC IgG1 monoclonal (Miltenyi Biotec), anti-CD45-FITC IgG2aκ monoclonal (Miltenyi Biotec), and anti-CD11b-FITC IgG2b monoclonal (Thermo Fisher Scientific). Cells were purified using a BD FACSAria III (Becton Dickinson, Sydney, Australia), centrifuged (300 g; 5 minutes) and immediately processed for RNA, protein collection or cell culture. Cells were cultured in Medium 199 (Thermo Fisher Scientific) with 10% fetal bovine serum (Interpath; Sydney, Australia), 1% Penicillin/Streptomycin (Thermo Fisher Scientific), 0.1% Fungizone (Thermo Fisher Scientific), 10 μM ROCK inhibitor (Sigma), SCF (25 ng/mL), DLL-1 (50 ng/mL), PDGF-BB (10 ng/mL), FGF-2 (20 ng/mL), NT-3 (20 ng/mL), and BDNF (50 ng/mL) from Miltenyi Biotec, plus ITS (1X), IGF-1 (100 ng/mL), and EGF (100 ng/mL) from Lonza (Sydney, Australia). Cultures were fixed (4% paraformaldehyde, room temperature, 15 minutes) and permeabilized (0.5% Triton X-100/PBS, room temperature, 10 minutes) prior to immunofluorescence as described above. Images were captured with the LSM-800 laser scanning confocal microscope (Zeiss) using the 405 nm, 488 nm, and 561 nm emission filters.

RNA Purification, Real-time Polymerase Chain Reaction, Bulk RNA-sequencing, and Gene Ontology Analyses

Total RNA was purified using NucleoSpin RNA Plus XS kits (Scientifix, Melbourne, Australia). RNA quality was assessed using the Bioanalyser (RNA 6000 Pico kit; Agilent Technologies, Melbourne, Australia). All RNA samples were from non-diabetic samples and had a Bioanalyser RNA integrity number ≥ 7.5. Reverse transcription was performed using Tetro Reverse Transcriptase (Bioline, Sydney, Australia), before real-time polymerase chain reaction (PCR) on a Mx3005P System with MxPro software (Agilent Technologies) using the following TaqMan primers (Thermo Fisher Scientific): ANO1 (Hs00216121_m1); CACNA1H (Hs01103527_m1); KIT (Hs00174029_m1); CD68 (Hs00154355_m1); CPA3 (Hs00157019_m1); *UCHL1* (Hs00985154_m1); DES (Hs00157258_m1); ACTG2 (Hs01123712_m1); and GAPDH (Hs02758991_g1). Relative gene expression was calculated using the $2^{-\Delta\Delta C_T}$ method.[17] Significance was analyzed using a parametric Student's *t* test.

Bulk RNA-seq was performed by the Monash Health Translation Precinct Medical Genomics Facility (Melbourne, Australia) on a NextSeq550 (Illumina, San Diego, USA) using the V2 High Output kit.[18] Paired-end sequence reads were de-multiplexed, mapped to the human genome (hg38) with STAR and de-duplicated. Read counts were calculated using featureCounts and converted to transcripts per kilobase million. Gene ontology (GO) biological process analyses were performed using the functional annotation tool on DAVID.[19] Only significant GO terms were reported (Benjamini *P*-value < 0.05).

Mass Spectrometry Analysis

Samples were lysed in 0.5% RapiGest (Waters, Sydney, Australia) in 50 mM NH_4HCO_3, followed by 3 freeze-thaw cycles in liquid nitrogen.[20] Samples were then reduced (60℃, 1 hour; 5 mM dithiothreitol; Chem-Supply), alkylated (room temperature, 1 hour; 15 mM iodoacetamide; Merck, Sydney, Australia) and proteolyzed (37℃, overnight; Trypsin Gold; Promega, Sydney, Australia). Peptides were purified using Oasis HLB solid-phase extraction cartridges (Waters) and resuspended in 0.1% aqueous formic acid (Sigma). Mass spectrometry was performed on a nanoAcquity UPLC connected to a SYNAPT G2-Si (HDMS) spectrometer (Waters). Data was processed using MassLynx software (Waters) and Progenesis QI for Proteomics (version 4.1; Waters). Peptides were searched against the UniProt human protein FASTA data-

base, with variable modifications: carbamidomethyl (C), deamidation (N and Q), oxidation (M), and propionamide (C). Relative protein quantitation was performed with the Hi-N method using the top 3 peptides. Proteins were identified if expressed in at least 2 technical replicates in at least 1 sample. Protein interaction networks with a minimum interaction score of 0.4 were generated using the human STRING database (v11.0).[21]

Results

Visualization and Isolation of Interstitial Cells of Cajal From Human Gastric Muscle Tissue

To confirm the presence of ICC in the patient samples, immunofluorescence was performed using antibodies against ANO1 and KIT (Fig. 1A). Co-localized ANO1^{+}/KIT^{+} staining was observed

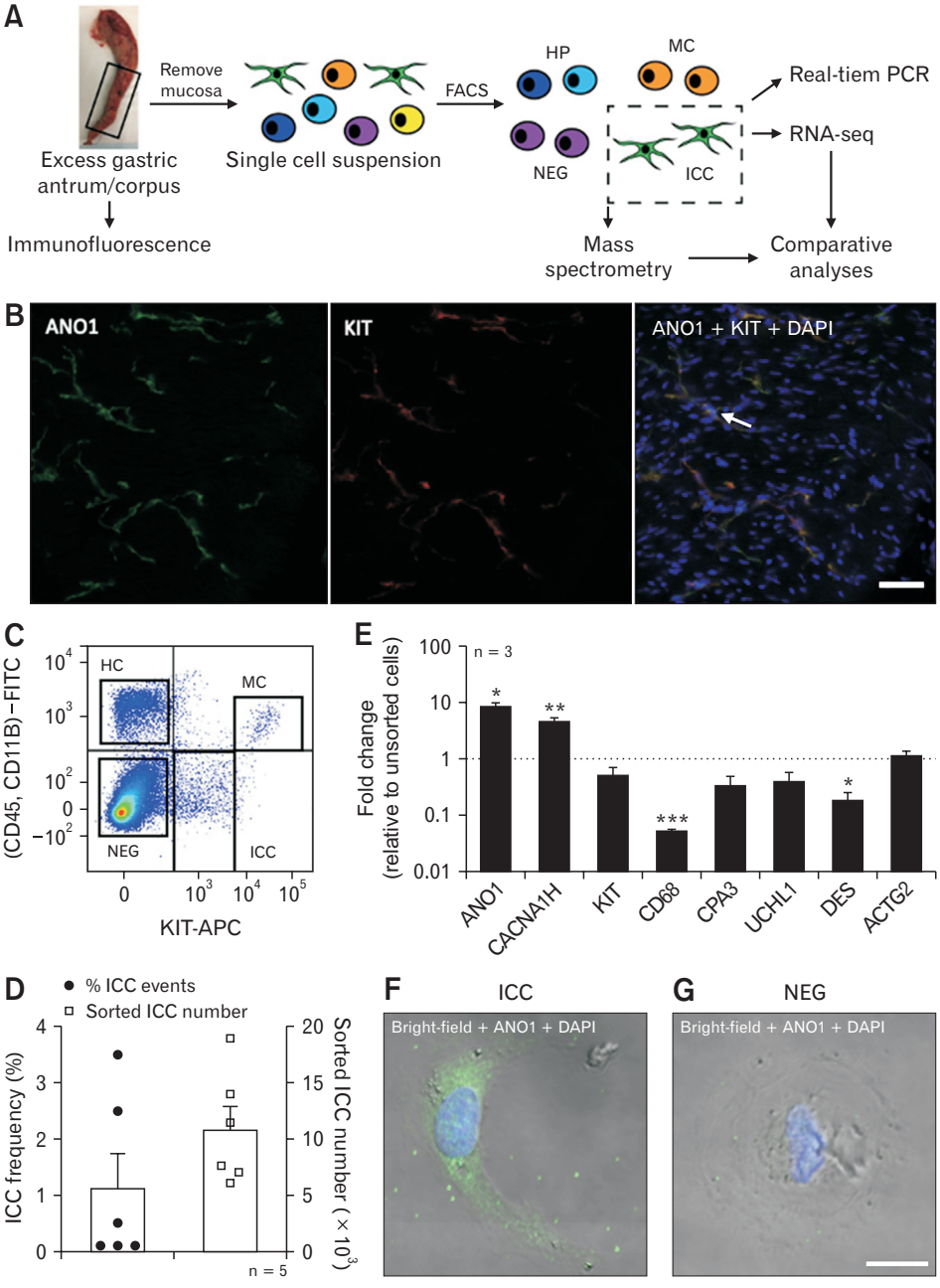

Figure 1. Immunofluorescent labelling and purification of interstitial cells of Cajal (ICC) in human gastric muscle tissue. (A) Workflow used to investigate primary human ICC from sleeve gastrectomy samples. (B) Co-localization of calcium-activated chloride channel anoctamin-1 (ANO1) (green; left) and receptor tyrosine kinase (KIT) (red; middle) in sectioned human gastric tissue. Merged image (right) shows ANO1^{+}/KIT^{+} labelled ICC (arrow) with DAPI staining indicating cell nuclei (blue). Scale bar = 50 μm. (C) Representative flow cytometry plot showing key cell populations: negative cells (NEG; KIT^{-}/CD45^{-}/CD11B^{-}), hematopoietic cells (HCs; KIT^{-}/CD45^{+}/CD11B^{+}), mast cells (MCs; KIT^{high}/CD45^{+}/CD11B^{+}), and ICC (KIT^{low}/CD45^{-}/CD11B^{-}). (D) ICC frequency and sorted ICC numbers. Each dot represents a patient sample. (E) Real-time polymerase chain reaction data for the ICC population versus the unsorted population using cell-type markers (*ANO1, CACNA1H, KIT, CD68, CPA3, UCHL1, DES*, and *ACTG2*; data normalized to *GAPDH* and expressed as mean fold change ± standard error of the mean relative to unsorted cells—dotted line). Significant differences compared to unsorted cells: $^{*}P < 0.05$, $^{**}P < 0.01$, $^{***}P < 0.001$. (F, G) Merged (bright-field, ANO1 fluorescence in green and DAPI nuclear stain in blue) images of purified human gastric ICC (F) and NEG (G) after 2 days in culture. Scale bar = 10 μm.

in cells throughout the muscle (Fig. 1B), indicative of ICC.[7,16,22] While differences between ICC populations have been reported between the human gastric antrum, corpus and fundus,[23] it was difficult to distinguish between these regions in the cryosections presented here, so any regional differences in ICC were not described.

Subsequent FACSorting-based purification of cell populations from dissociated gastric muscle was performed using antibodies against KIT and the hematopoietic markers, CD45 and CD11B (Fig. 1C). Four cell populations were observed: (1) negative cells (NEG; $KIT^-/CD45^-/CD11B^-$), (2) hematopoietic cells (HCs; $KIT^-/CD45^+/CD11B^+$), (3) MCs ($KIT^{high}/CD45^+/CD11B^+$), and (4) ICC ($KIT^{low}/CD45^-/CD11B^-$). Notably, the cell populations obtained were similar to those previously seen with FACSorting of primary human gastric ICC.[15,16] On average, the frequency of ICC was $1.1 \pm 0.6\%$ of the total live cells, and $1.1 \pm 0.2 \times 10^4$ ICC were obtained after sorting (Fig. 1D).

Real-time PCR analyses of the MC and HC populations showed (as predicted) enriched expression of mast cell[24,25] and macrophage/monocyte[26] markers, respectively (Supplementary Figure A and B). Conversely, PCR analysis of the $KIT^{low}/CD45^-/CD11B^-$ cells revealed a gene expression pattern consistent with ICC (Fig. 1E).[7,10,27] Compared to unsorted cells, the $KIT^{low}/CD45^-/CD11B^-$ ICC showed: 9-fold increased *ANO1* expression ($P < 0.05$); 5-fold increase in *CACNA1H* ($P < 0.01$), thought to be involved in initiating ICC slow wave contractions, and expressed in both ICC and smooth muscle cells;[28,29] unchanged *KIT* expression; and $>$ 10-fold reduced expression of the hematopoietic cell marker *CD68* ($P < 0.001$). The $KIT^{low}/CD45^-/CD11B^-$ cells also showed trends for reduced expression of the mast cell marker *CPA3* and the neuronal marker *UCHL1* ($P = 0.130$ and $P = 0.120$, respectively). For *UCHL1*, this matched previous scRNA-seq data from purified human gastric ICC[16] and publicly available scRNA-seq data from fetal intestinal ICC.[30] The detection of *CPA3* in the PCR data also suggests a small number of MCs ($KIT^{high}/CD45^+/CD11B^+$) may have been captured within the ICC gate. Compared to the unsorted cells, and consistent with bulk RNA-seq data from mouse jejunum/colon ICC[14] and scRNA-seq data from intestinal ICC,[30] the FACSorted ICC population showed a $>$ 4-fold reduction ($P < 0.05$) in the smooth muscle marker *DES* (Fig. 1E), but similar levels of the smooth muscle cell-expressed gene *ACTG2*. In contrast, compared to unsorted cells, the unsorted gastric smooth muscle tissue showed a different gene expression pattern characteristic of smooth muscle cells[14,30,31] ie, ~7-fold higher expression of *DES*, and ~21-fold higher expression of *ACTG2* compared to *ANO1* (Supplementary Figure C).

To further assess whether the $KIT^{low}/CD45^-/CD11B^-$ cells represented ICC, the cells were cultured in a medium containing growth factors that bind receptors highly-expressed in the bulk RNA-seq data. Immunostaining after 2 days of culture showed ANO1 staining on the sorted $KIT^{low}/CD45^-/CD11B^-$ cells (Fig. 1F), but not on the sorted KIT-/$CD45^-/CD11B^-$ NEG (Fig. 1G). This aligned with previous data that showed 95% of the $KIT^{low}/CD45^-/CD11B^-$ cells exhibited ANO1 protein expression.[16] Collectively, these data are consistent with the vast majority of $KIT^{low}/CD45^-/CD11B^-$ cells representing primary human gastric ICC.

RNA-sequencing Analysis of Human Gastric Interstitial Cells of Cajal

Bulk RNA-seq analysis of the FACSorted $KIT^{low}/CD45^-/CD11B^-$ ICC identified 3878 expressed genes (Supplementary Table 1), including *ANO1* and *KIT*; the relatively low expression for these genes is consistent with other human ICC transcriptomic datasets.[15,30] GO analysis of the expressed genes revealed biological process terms consistent with ICC pacemaker activity (Supplementary Table 2), such as "relaxation of cardiac muscle" and "regulation of release of sequestered calcium ion into cytosol by sarcoplasmic reticulum."[32-34]

The bulk RNA-seq data was then compared to scRNA-seq gene expression profiles previously generated from purified primary human gastric ICC.[16] This comparison revealed 3387 genes (87%) were expressed by ICC in both the bulk and scRNA-seq datasets. Further comparison showed the bulk ICC RNA-seq data overlapped with 75% of previously identified scRNA-seq ICC marker genes, but only 50% of scRNA-seq HC marker genes. GO analysis of the overlapping bulk ICC RNA-seq expressed genes and scRNA-seq ICC marker genes revealed top GO terms consistent with ICC functions, including: "regulation of muscle contraction"; "ATP synthesis coupled electron transport"; and "calcium ion transport from endoplasmic reticulum to cytosol" (Table 1). In contrast, none of these ICC-associated terms were identified when comparing the bulk ICC RNA-seq genes with the scRNA-seq HC marker genes (Supplementary Table 3). Overall, these bulk RNA-seq analyses provide further support for the $KIT^{low}/CD45^-/CD11B^-$ cells being human gastric ICC.

Comparison of Fluorescence-activated Cell-sorted Human Interstitial Cells of Cajal Bulk RNA-sequencing and Mass Spectrometry Data

Shotgun proteomics based-mass spectrometry analysis was also performed on the $KIT^{low}/CD45^-/CD11B^-$ ICC to investigate

Table 1. Top 30 Gene Ontology Terms From the Overlapping Interstitial Cells of Cajal Bulk RNA-sequencing Expressed Genes and Single-cell RNA-sequencing Marker Genes

GO ID	Term	Benjamini *P*-value
GO:0006937	Regulation of muscle contraction	7.02E-06
GO:0019932	Second-messenger-mediated signaling	2.22E-04
GO:0072001	Renal system development	9.16E-04
GO:0001822	Kidney development	1.16E-03
GO:0001655	Urogenital system development	1.42E-03
GO:0042773	ATP synthesis coupled electron transport	1.42E-03
GO:0007507	Heart development	1.92E-03
GO:0070527	Platelet aggregation	2.35E-03
GO:0072006	Nephron development	2.54E-03
GO:0006120	Mitochondrial electron transport, NADH to ubiquinone	2.76E-03
GO:0030168	Platelet activation	2.76E-03
GO:0022904	Respiratory electron transport chain	4.42E-03
GO:0055001	Muscle cell development	4.73E-03
GO:0030900	Forebrain development	4.73E-03
GO:0009887	Organ morphogenesis	4.92E-03
GO:0034109	Homotypic cell-cell adhesion	5.18E-03
GO:0055002	Striated muscle cell development	6.28E-03
GO:0032835	Glomerulus development	7.24E-03
GO:0010001	Glial cell differentiation	7.25E-03
GO:0006163	Purine nucleotide metabolic process	8.65E-03
GO:0006939	Smooth muscle contraction	9.24E-03
GO:1904062	Regulation of cation transmembrane transport	1.03E-02
GO:0031032	Actomyosin structure organization	1.11E-02
GO:0009259	Ribonucleotide metabolic process	1.23E-02
GO:1903514	Calcium ion transport from endoplasmic reticulum to cytosol	1.23E-02
GO:0014808	Release of sequestered calcium ion into cytosol by sarcoplasmic reticulum	1.23E-02
GO:0022604	Regulation of cell morphogenesis	1.36E-02
GO:0010959	Regulation of metal ion transport	1.41E-02
GO:0010880	Regulation of release of sequestered calcium ion into cytosol by sarcoplasmic reticulum	1.41E-02
GO:0019693	Ribose phosphate metabolic process	1.65E-02

GO, gene ontology.

whether the RNA-seq findings were replicated at the protein level. In total, 234 proteins were identified (Supplementary Table 4). Neither KIT nor ANO1 proteins were identified in the FACSorted ICC, as predicted based on both the low number of ICC captured and the detection sensitivity for lower abundance proteins in shotgun proteomics.[35] Notably, mass spectrometry analysis of dissected whole human gastric smooth muscle tissue showed high confidence scores for key smooth muscle cell-specific marker proteins, including DES and MYH11 (Supplementary Table 5). The absence of large numbers of peptides for these highly abundant smooth muscle cell proteins in the $KIT^{low}/CD45^{-}/CD11B^{-}$ ICC population suggests few, if any, smooth muscle cells were captured in the $KIT^{low}/CD45^{-}/CD11B^{-}$ ICC population.

Subsequent GO analysis of the ICC-expressed proteins (Table 2) revealed terms consistent with published ICC ultrastructural characterization studies (ie, presence of numerous intermediate filaments)[36] as well as ICC-associated functions (eg, "regulation of cell motility").[1] In contrast, GO analysis of the proteins expressed in whole human gastric smooth muscle tissue showed different terms – more related to smooth muscle cells than ICC—including "muscle organ development" and "collagen fibril organization"[31,37] (Supplementary Table 6). Comparison of the ICC-expressed proteins and ICC bulk RNA-seq datasets revealed ~44% overlap—including proteins associated with GI motility (such as caveolin 1 [CAV1] and myosin light chain kinase [MYLK]).[38,39] GO analysis of these overlapping ICC-expressed genes/proteins revealed terms related to

ICC-associated functions, including "regulation of muscle contraction" and "regulation of cation transmembrane transport" (Supplementary Table 7).[34,38,39] Overall, the mass spectrometry data are consistent with the KIT^{low}/CD45^{-}/CD11B^{-} population containing purified ICC.

Predicted Interstitial Cells of Cajal Protein Interaction Networks

Additional GO analyses—performed on the overlap between the bulk ICC RNA-seq, scRNA-seq, and mass spectrometry data (Table 3)—revealed terms consistent with ICC pacemaker activity. This included "regulation of muscle contraction" and "positive regulation of ion transport."[32-34] STRING-based analysis of the ICC-expressed genes/proteins associated with these 2 GO terms (Fig. 2A and 2B) revealed CAV1—a critical regulator of mouse ICC pacing and contractions[38]—to be present in both networks.

Table 2. Gene Ontology Analysis of the Proteins Detected Within the Fluorescence-Activated Cell Sorted Primary Human Interstitial Cells of Cajal (KIT^{low}/CD45^{-}/CD11B^{-}) Population

GO ID	Term	Benjamini *P*-value
GO:0045104	Intermediate filament cytoskeleton organization	3.92E-08
GO:0045109	Intermediate filament organization	1.63E-06
GO:0030036	Actin cytoskeleton organization	5.17E-06
GO:0030049	Muscle filament sliding	7.55E-05
GO:0031032	Actomyosin structure organization	2.44E-04
GO:0007015	Actin filament organization	2.71E-04
GO:0048513	Animal organ development	3.47E-04
GO:0070252	Actin-mediated cell contraction	3.53E-04
GO:0016477	Cell migration	9.38E-04
GO:0008360	Regulation of cell shape	5.92E-03
GO:0055002	Striated muscle cell development	2.07E-02
GO:0048468	Cell development	2.27E-02
GO:0000902	Cell morphogenesis	2.71E-02
GO:0030239	Myofibril assembly	3.34E-02
GO:0043588	Skin development	3.34E-02
GO:0055001	Muscle cell development	3.34E-02
GO:0007044	Cell-substrate junction assembly	4.17E-02
GO:0014706	Striated muscle tissue development	4.17E-02
GO:0030855	Epithelial cell differentiation	4.17E-02
GO:0051146	Striated muscle cell differentiation	4.17E-02
GO:0055013	Cardiac muscle cell development	4.17E-02
GO:2000145	Regulation of cell motility	4.17E-02
GO:0030334	Regulation of cell migration	4.31E-02
GO:0055006	Cardiac cell development	4.31E-02
GO:0042692	Muscle cell differentiation	4.94E-02

GO, gene ontology.

Discussion

Normal GI peristaltic activity relies on ICC to generate and propagate slow waves to smooth muscle cells.[40-42] Most ICC characterization studies have been performed on mouse GI tissue from normal and/or genetically-modified mice.[1,13] Increased knowledge of human ICC characteristics will facilitate development of new

Table 3. Gene Ontology Terms From the Interstitial Cells of Cajal-expressed Proteins That Overlap With the Bulk RNA-sequencing Expressed Genes and Interstitial Cells of Cajal Single-cell RNA-sequencing Marker Genes

GO ID	Term	Benjamin *P*-value
GO:0030036	Actin cytoskeleton organization	2.67E-07
GO:0007015	Actin filament organization	1.42E-05
GO:0070252	Actin-mediated cell contraction	1.29E-04
GO:0006937	Regulation of muscle contraction	7.46E-04
GO:0007517	Muscle organ development	2.32E-03
GO:0043270	Positive regulation of ion transport	2.32E-03
GO:0014706	Striated muscle tissue development	2.32E-03
GO:0030049	Muscle filament sliding	2.98E-03
GO:0051146	Striated muscle cell differentiation	3.80E-03
GO:0016477	Cell migration	4.37E-03
GO:0055002	Striated muscle cell development	4.37E-03
GO:0031032	Actomyosin structure organization	5.17E-03
GO:0000902	Cell morphogenesis	5.17E-03
GO:0055001	Muscle cell development	5.17E-03
GO:0048468	Cell development	5.95E-03
GO:0006941	Striated muscle contraction	5.95E-03
GO:0010959	Regulation of metal ion transport	6.65E-03
GO:0042692	Muscle cell differentiation	1.08E-02
GO:1904062	Regulation of cation transmembrane transport	1.46E-02
GO:0048513	Animal organ development	1.65E-02
GO:0046716	Muscle cell cellular homeostasis	1.65E-02
GO:0072358	Cardiovascular system development	1.96E-02
GO:0072359	Circulatory system development	1.96E-02
GO:0030334	Regulation of cell migration	2.10E-02
GO:0051271	Negative regulation of cellular component movement	2.32E-02
GO:2000145	Regulation of cell motility	2.82E-02
GO:0051017	Actin filament bundle assembly	3.08E-02
GO:0045055	Regulated exocytosis	3.08E-02
GO:0010927	Cellular component assembly involved in morphogenesis	3.21E-02
GO:0043269	Regulation of ion transport	4.47E-02

GO, gene ontology.
Terms related to interstitial cells of Cajal functions are highlighted in gray.

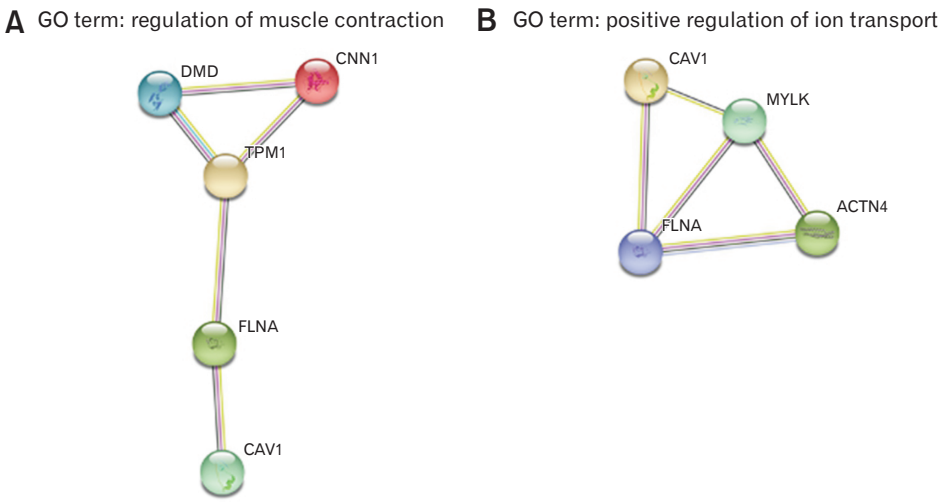

Figure 2. STRING-based protein interaction networks from interstitial cells of Cajal-expressed proteins associated with the Gene Ontology terms identified in Table 3: "regulation of muscle contraction" (A) and "positive regulation of ion transport" (B). Each node represents a protein. Edges represent protein-protein interactions: light blue = known interaction, from curated database; purple = known interaction, experimentally determined; red = predicted interaction, gene fusions; light green = other interaction, text-mining; black = other interaction, co-expression; blue = other interaction, protein homology. Some proteins are expressed in ICC: Duchenne muscular dystrophy (DMD) encodes dystrophin protein, which showed modified ICC morphology and gastric dysmotility when knocked out in mice[48,49]; caveolin 1 (CAV1) is a key scaffolding protein of caveolae on cell membranes essential for normal calcium handling in pacing and contractions in the mouse small intestine;[38,50,51] and myosin light chain kinase (MYLK) is a kinase protein, important in gastric smooth muscle contraction.[14,31]

treatments for GI motility disorders, with the potential to improve the quality of life for millions of patients worldwide.[13]

Here, primary human gastric muscle tissues—containing ANO1- and KIT-expressing ICC—were dissociated prior to capture of KIT^{low}/CD45^{-}/CD11B^{-} cells via flow cytometry. The FACSorting profiles obtained were similar to previously generated[16] and published[15] profiles for purified human gastric ICC. Real-time PCR analysis showed the KIT^{low}/CD45^{-}/CD11B^{-} cells had high expression of ICC-related genes (eg, > 9-fold enrichment in *ANO1*), and low expression of immune, neural cell and smooth muscle cell-associated genes (*CPA3/CD68*, *UCHL1*, and *DES/ACTG2*, respectively). Immunofluorescence analysis of these cells after 2 days in culture showed ANO1 protein, consistent with the ICC phenotype[7,27] and our previous data.[16] Collectively, these data provide strong and complementary evidence indicating the KIT^{low}/CD45^{-}/CD11B^{-} cells are an enriched population of human gastric ICC, with little evidence for large-scale contamination by smooth muscle cells or other cell types (though some *CPA3*-expressing cells might be present).

Bulk RNA-sequencing Detects Genes and Gene Ontology Terms Consistent With Interstitial Cells of Cajal

Characterization of the KIT^{low}/CD45^{-}/CD11B^{-} ICC using bulk RNA-seq revealed a gene expression profile more similar to human gastric ICC than gastric HCs. While *ANO1* and *KIT* were expressed at low levels, this is consistent with low expression levels observed for these genes, both in our previously generated ICC scRNA-seq data[16] and in the human fetal gut cell atlas ICC scRNA-seq data.[30] GO analyses of the bulk ICC RNA-seq data revealed terms associated with smooth muscle contraction and ion transport – key biological processes involved in ICC pacemaker activity and GI motility.[32-34] Several of the genes associated with these GO terms have been observed to be important in ICC pacemaker activity. This includes: *ATP1A2*, a sodium/potassium-transporting ATPase subunit expressed in mouse ICC;[11,14,43] *PRKG1*, a cGMP-dependent serine/threonine kinase expressed in mouse ICC that regulates GI smooth muscle contraction;[44,45] and *GUCY1A3, GUCY1B3,* and *MRVI1*, key signaling genes expressed in mouse ICC and important for nitric oxide-mediated smooth muscle relaxation within the GI tract.[46]

Mass Spectrometry and Associated Gene Ontology Analyses Complement the Bulk RNA-sequencing Data

The mass spectrometry data generated from the KIT^{low}/CD45^{-}/CD11B^{-} ICC showed ~44% overlap with the bulk RNA-seq dataset. This is not unexpected given that RNA levels do not necessarily predict protein levels.[47] While the real-time PCR data showed enrichment of *ANO1* transcripts in the purified ICC, the mass spectrometry data showed no ANO1 or KIT peptides. However, this was predicted based on both the low number of cells captured and the difficulty in detecting membrane proteins in whole-cell shotgun proteomics.[35] Notably, high levels of gene and protein expression for highly abundant smooth muscle cell markers, such as DES and MYH11, were not observed in the purified ICC population. This finding further supports the FACSorted ICC population not containing large numbers of smooth muscle cells.

GO analysis of the proteins/genes that overlapped between the mass spectrometry and RNA-seq datasets revealed terms consistent with ICC functions and associated with calcium sensitization in GI smooth muscle contraction, for example, "regulation of muscle contraction" and "positive regulation of ion transport." Moreover, highly-expressed proteins identified in both the mass spectrometry and bulk RNA-seq data have functions consistent with ICC biology. This includes: Duchenne muscular dystrophy (DMD), encodes the dystrophin protein, which showed altered ICC morphology and gastric dysmotility when knocked out in mice;[48,49] CAV1, a key scaffolding protein of caveolae on cell membranes essential for normal calcium handling in pacing and contractions in the mouse small intestine;[38,50,51] and MYLK, which is highly expressed in both mouse smooth muscle cells and ICC.[14,31] Conspicuously, both CAV1 and MYLK proteins are key regulators of calcium sensitization in GI smooth muscle contraction, though the exact cell types in which these proteins are involved have not been fully elucidated.[38,39,52] Thus, detection of CAV1 and MYLK in the KIT^{low}/CD45^{-}/CD11B^{-} ICC population suggests these proteins play some role in regulating calcium levels and pacemaker activity in human ICC. As discussed below, this is consistent with both Cav1- and Mylk-knockout mice having abnormal GI physiology and/or abnormal GI motility.

Predicted Interstitial Cells of Cajal Protein Networks Provide Insights Into Human Interstitial Cells of Cajal Biology

The STRING-based protein networks predicted here from the overlapping mass spectrometry and RNA-seq data provide candidate molecular hypotheses for how human ICC might regulate GI smooth muscle contraction. For instance, it has been suggested that CAV1—expressed in mouse small intestinal ICC[50,51]—and caveolae are required for normal calcium handling within ICC. Mouse *Cav1* gene knockouts display abnormal ICC pacing frequencies[38] and impaired smooth muscle relaxation[53] within the small intestine. Thus, the combined RNA-seq data, mass spectrometry data, GO analyses and STRING networks presented here all suggest CAV1 and its downstream mediators might act as regulating sites for pacemaker activity and ion transport in human gastric ICC—thereby, controlling smooth muscle contraction and/or relaxation. While CAV1 and MYLK are also expressed in smooth muscle cells,[31,50] the low gene expression levels of key smooth muscle cell marker proteins seen in the FACSorted ICC population here and elsewhere[16] indicate few, if any, smooth muscle cells were captured in the KIT^{low}/CD45^{-}/CD11B^{-} population. Additionally, the KIT^{low}/CD45^{-}/CD11B^{-} cells expressed ANO1 protein (detected via immunofluorescence), whereas the other FACSorted cell populations did not. Collectively, these data suggest CAV1-associated networks may regulate pacemaker activity and ion transport in human gastric ICC via the interaction between caveolae and ion channels, which is consistent with the single-cell RNA-seq analysis of human gastric ICC.[16] Further investigations of this predicted network will help determine their functional relevance in ICC-mediated regulation gastric smooth muscle contraction. For example, the effect of activators or inhibitors on these candidate proteins, such as incadronate for CAV1[54] and lithium for MYLK,[55] to explore their impact on pacemaker activity using electrophysiology and/or calcium imaging on cultured KIT^{low}/CD45^{-}/CD11B^{-}ICC, as has been similarly conducted using carbachol in cultured mouse ICC from the small intestine.[56] Such studies could have major clinical implications in identifying candidate small molecules capable of altering ICC electrophysiology, which in turn may lead to clinical trials investigating the potential for small molecules to improve pacemaker activity in patients with functional GI motility disorders where ICC networks are altered (eg, gastroparesis).

Given that it was not possible to access gastric tissue from healthy (ie, non-obese) individuals, it should also be noted that it is assumed the sleeve gastrectomy samples performed for morbid obesity—from which the ICC were purified—were "normal." Future studies could focus on other potential sources of ICC human GI tissue, such as recently deceased cadavers from non-obese individuals or colon tissue from colorectal cancer resections. While these ICC sources have their own inherent and important caveats, it

nevertheless may be informative to compare the transcriptional and protein profiles from these alternative sources to the data obtained here to evaluate common molecular mechanisms across the different human ICC types and sources.

In conclusion, despite the low numbers of ICC accessible from human gastric tissue samples—a limitation also experienced in previous studies of human ICC[13,16]—the data presented here from complementary RNA-seq and mass spectrometry analyses are consistent with the known role of ICC in GI motility. The overlapping findings between these new datasets and previous ICC scRNA-seq data[16]—together with ANO1 protein expression and the lack of strong evidence for smooth muscle cells within the KIT^{low}/$CD45^{-}$/$CD11B^{-}$ population—supports the reliability of these new results to provide new insights into human gastric ICC biology. These data will provide a useful framework for future functional studies aimed at testing new molecular hypotheses of ICC pacemaker activity (such as the role of CAV1 and MYLK in ICC). This could include inhibitor-based electrophysiology studies using FACSorted primary human ICC—with the potential to help identify candidate drug targets and/or drugs for treating GI motility disorders.

Supplementary Materials

Note: To access the supplementary figure and tables mentioned in this article, visit the online version of *Journal of Neurogastroenterology and Motility* at http://www.jnmjournal.org/, and at https://doi.org/10.5056/jnm22078.

Acknowledgements: The authors acknowledge that the data presented in this study was acquired by personnel and/or instruments at the Flow Cytometry Facility (Mark Wainwright Analytical Center), Ramaciotti Centre for Genomics, Monash Health Translation Precinct Medical Genomics Facility and WSU Mass Spectrometry Facility.

Financial support: This work was funded by Western Sydney University and Australian Rotary Health Postgraduate Research Award.

Conflicts of interest: None.

Author contributions: Daphne Foong and Michael D O'Connor conceptualized and designed the research; Ali Zarrouk provided the human tissue samples; Daphne Foong, Meena Mikhael Jerry Zhou, Xiaodong Liu, Jan Schröder, and Jose Polo conducted the experiments; Daphne Foong, Meena Mikhael, and Michael D O'Connor interpreted the data and drafted the manuscript; and Daphne Foong, Meena Mikhael, Jerry Zhou, Xiaodong Liu, Jan Schröder, Jose Polo, Vincent Ho, and Michael D O'Connor reviewed the manuscript. All authors have read and agreed to the manuscript.

References

1. Blair PJ, Rhee PL, Sanders KM, Ward SM. The significance of interstitial cells in neurogastroenterology. J Neurogastroenterol Motil 2014;20:294-317.
2. Farrugia G. Interstitial cells of cajal in health and disease. Neurogastroenterol Motil 2008;20(suppl):54-63.
3. Streutker CJ, Huizinga JD, Driman DK, Riddell RH. Interstitial cells of cajal in health and disease. Part I: normal ICC structure and function with associated motility disorders. Histopathology 2007;50:176-189.
4. Maeda H, Yamagata A, Nishikawa S, et al. Requirement of c-kit for development of intestinal pacemaker system. Development 1992;116:369-375.
5. Torihashi S, Horisawa M, Watanabe Y. c-Kit immunoreactive interstitial cells in the human gastrointestinal tract. J Auton Nerv Syst 1999;75:38-50.
6. Torihashi S, Ward SM, Nishikawa S, Nishi K, Kobayashi S, Sanders KM. c-kit-dependent development of interstitial cells and electrical activity in the murine gastrointestinal tract. Cell Tissue Res 1995;280:97-111.
7. Gomez-Pinilla PJ, Gibbons SJ, Bardsley MR, et al. Ano1 is a selective marker of interstitial cells of cajal in the human and mouse gastrointestinal tract. Am J Physiol Gastrointest Liver Physiol 2009;296:G1370-G1381.
8. Zhu MH, Kim TW, Ro S, et al. A Ca^{2+}-activated Cl^{-} conductance in interstitial cells of cajal linked to slow wave currents and pacemaker activity. J Physiol 2009;587(Pt 20):4905-4918.
9. Ordög T, Redelman D, Horowitz NN, Sanders KM. Immunomagnetic enrichment of interstitial cells of cajal. Am J Physiol Gastrointest Liver Physiol 2004;286:G351-G360.
10. Ordög T, Redelman D, Miller LJ, et al. Purification of interstitial cells of cajal by fluorescence-activated cell sorting. Am J Physiol Cell Physiol 2004;286:C448-C456.
11. Chen H, Ordög T, Chen J, et al. Differential gene expression in functional classes of interstitial cells of cajal in murine small intestine. Physiol Genomics 2007;31:492-509.
12. Chen H, Redelman D, Ro S, Ward SM, Ordög T, Sanders KM. Selective labeling and isolation of functional classes of interstitial cells of cajal of human and murine small intestine. Am J Physiol Cell Physiol 2007;292:C497-C507.
13. Foong D, Zhou J, Zarrouk A, Ho V, O'Connor MD. Understanding the biology of human interstitial cells of cajal in gastrointestinal motility. Int J Mol Sci 2020;21:4540.
14. Lee MY, Ha SE, Park C, et al. Transcriptome of interstitial cells of cajal reveals unique and selective gene signatures. PLoS One 2017;12:e0176031.
15. Tang CM, Lee TE, Syed SA, et al. Hedgehog pathway dysregulation contributes to the pathogenesis of human gastrointestinal stromal

tumors via GLI-mediated activation of KIT expression. Oncotarget 2016;7:78226-78241.
16. Foong D, Liyanage L, Zhou J, Zarrouk A, Ho V, O'Connor MD. Single-cell RNA sequencing predicts motility networks in purified human gastric interstitial cells of cajal. Neurogastroenterol Motil 2022;34:e14303.
17. Livak KJ, Schmittgen TD. Analysis of relative gene expression data using real-time quantitative PCR and the $2^{-\Delta\Delta CT}$ Method. Methods 2001;25:402-408.
18. Grubman A, Choo XY, Chew G, et al. Mouse and human microglial phenotypes in Alzheimer's disease are controlled by amyloid plaque phagocytosis through Hif1α. bioRxiv 2019:639054.
19. Huang da W, Sherman BT, Lempicki RA. Systematic and integrative analysis of large gene lists using DAVID bioinformatics resources. Nat Protoc 2009;4:44-57.
20. Murphy P, Kabir MH, Srivastava T, et al. Light-focusing human microlenses generated from pluripotent stem cells model lens development and drug-induced cataract *in vitro*. Development 2018;145:dev155838.
21. Szklarczyk D, Gable AL, Lyon D, et al. STRING v11: protein-protein association networks with increased coverage, supporting functional discovery in genome-wide experimental datasets. Nucleic Acids Res 2019;47:D607-D613.
22. Hwang SJ, Blair PJ, Britton FC, et al. Expression of anoctamin 1/TMEM16A by interstitial cells of cajal is fundamental for slow wave activity in gastrointestinal muscles. J Physiol 2009;587(Pt 20):4887-4904.
23. Ibba Manneschi L, Pacini S, Corsani L, Bechi P, Faussone-Pellegrini MS. Interstitital cells of cajal in the human stomach: distribution and relationship with enteric innervation. Histol Histopathol 2004;19:1153-1164.
24. Lammie A, Drobnjak M, Gerald W, Saad A, Cote R, Cordon-Cardo C. Expression of c-kit and kit ligand proteins in normal human tissues. J Histochem Cytochem 1994;42:1417-1425.
25. Reynolds DS, Gurley DS, Austen KF. Cloning and characterization of the novel gene for mast cell carboxypeptidase A. J Clin Invest 1992;89:273-282.
26. Chistiakov DA, Killingsworth MC, Myasoedova VA, Orekhov AN, Bobryshev YV. CD68/macrosialin: not just a histochemical marker. Lab Invest 2017;97:4-13.
27. Loera-Valencia R, Wang XY, Wright GW, Barajas-López C, Huizinga JD. Ano1 is a better marker than c-kit for transcript analysis of single interstitial cells of cajal in culture. Cell Mol Biol Lett 2014;19:601-610.
28. Gibbons SJ, Strege PR, Lei S, et al. The α_{1H} Ca^{2+} channel subunit is expressed in mouse jejunal interstitial cells of cajal and myocytes. J Cell Mol Med 2009;13:4422-4431.
29. Zheng H, Park KS, Koh SD, Sanders KM. Expression and function of a T-type Ca^{2+} conductance in interstitial cells of cajal of the murine small intestine. Am J Physiol Cell Physiol 2014;306:C705-C713.
30. Elmentaite R, Ross ADB, Roberts K, et al. Single-cell sequencing of developing human gut reveals transcriptional links to childhood crohn's disease. Dev Cell 2020;55:771-783, e5.
31. Lee MY, Park C, Berent RM, et al. Smooth muscle cell genome browser: enabling the identification of novel serum response factor target genes. PLoS One 2015;10:e0133751.
32. Zhu MH, Sung TS, O'Driscoll K, Koh SD, Sanders KM. Intracellular Ca^{2+} release from endoplasmic reticulum regulates slow wave currents and pacemaker activity of interstitial cells of cajal. Am J Physiol Cell Physiol 2015;308:C608-C620.
33. Ward SM, Ördög T, Koh SD, et al. Pacemaking in interstitial cells of cajal depends upon calcium handling by endoplasmic reticulum and mitochondria. J Physiol 2000;525(Pt 2):355-361.
34. Huizinga JD, Golden CM, Zhu Y, White EJ. Ion channels in interstitial cells of cajal as targets for neurotransmitter action. Neurogastroenterol Motil 2004;16(suppl 1):106-111.
35. Zubarev RA. The challenge of the proteome dynamic range and its implications for in-depth proteomics. Proteomics 2013;13:723-726.
36. Komuro T. Structure and organization of interstitial cells of cajal in the gastrointestinal tract. J Physiol 2006;576(Pt 3):653-658.
37. Perr HA, Grider JR, Mills AS, et al. Collagen production by human smooth muscle cells isolated during intestinal organogenesis. Anat Embryol (Berl) 1992;185:517-527.
38. Daniel EE, Eteraf T, Sommer B, Cho WJ, Elyazbi A. The role of caveolae and caveolin 1 in calcium handling in pacing and contraction of mouse intestine. J Cell Mol Med 2009;13:352-364.
39. He WQ, Peng YJ, Zhang WC, et al. Myosin light chain kinase is central to smooth muscle contraction and required for gastrointestinal motility in mice. Gastroenterology 2008;135:610-620.
40. Takaki M. Gut pacemaker cells: the interstitial cells of cajal (ICC). J Smooth Muscle Res 2003;39:137-161.
41. Huizinga JD, Lammers WJ. Gut peristalsis is governed by a multitude of cooperating mechanisms. Am J Physiol Gastrointest Liver Physiol 2009;296:G1-G8.
42. Ordög T, Ward SM, Sanders KM. Interstitial cells of cajal generate electrical slow waves in the murine stomach. J Physiol 1999;518(Pt 1):257-269.
43. Zheng H, Drumm BT, Zhu MH, et al. Na^{+}/Ca^{2+} exchange and pacemaker activity of interstitial cells of cajal. Front Physiol 2020;11:230.
44. Cobine CA, Sotherton AG, Peri LE, Sanders KM, Ward SM, Keef KD. Nitrergic neuromuscular transmission in the mouse internal anal sphincter is accomplished by multiple pathways and postjunctional effector cells. Am J Physiol Gastrointest Liver Physiol 2014;307:G1057-G1072.
45. Iino S, Horiguchi K, Nojyo Y, Ward SM, Sanders KM. Interstitial cells of cajal contain signalling molecules for transduction of nitrergic stimulation in guinea pig caecum. Neurogastroenterol Motil 2009;21:542-550, e12-13.
46. Sanders KM, Ward SM. Nitric oxide and its role as a non-adrenergic, non-cholinergic inhibitory neurotransmitter in the gastrointestinal tract. Br J Pharmacol 2019;176:212-227.
47. Wang X, Liu Q, Zhang B. Leveraging the complementary nature of RNA-Seq and shotgun proteomics data. Proteomics 2014;14:2676-2687.
48. Vannucchi MG, Zardo C, Corsani L, Faussone-Pellegrini MS. Interstitial cells of cajal, enteric neurons, and smooth muscle and myoid cells of the murine gastrointestinal tract express full-length dystrophin. Histochem Cell Biol 2002;118:449-457.
49. Vannucchi MG, Zizzo MG, Zardo C, et al. Ultrastructural changes in

the interstitial cells of cajal and gastric dysrhythmias in mice lacking full-length dystrophin (mdx mice). J Cell Physiol 2004;199:293-309.
50. Cho WJ, Daniel EE. Proteins of interstitial cells of cajal and intestinal smooth muscle, colocalized with caveolin-1. Am J Physiol Gastrointest Liver Physiol 2005;288:G571-G585.
51. Cho WJ, Daniel EE. Colocalization between caveolin isoforms in the intestinal smooth muscle and interstitial cells of cajal of the $Cav1^{+/+}$ and $Cav1^{-/-}$ mouse. Histochem Cell Biol 2006;126:9-16.
52. Perrino BA. Calcium sensitization mechanisms in gastrointestinal smooth muscles. J Neurogastroenterol Motil 2016;22:213-225.
53. El-Yazbi AF, Cho WJ, Boddy G, Daniel EE. Caveolin-1 gene knock-out impairs nitrergic function in mouse small intestine. Br J Pharmacol 2005;145:1017-1026.
54. Iguchi K, Matsunaga S, Nakano T, Usui S, Hirano K. Inhibition of caveolin-1 expression by incadronate in PC-3 prostate cells. Anticancer Res 2006;26:2977-2981.
55. Tang ZY, Liu ZN, Fu L, Chen DP, Ai QD, Lin Y. Effect of lithium on smooth muscle contraction and phosphorylation of myosin light chain by MLCK. Physiol Res 2010;59:919-926.
56. So KY, Kim SH, Sohn HM, et al. Carbachol regulates pacemaker activities in cultured interstitial cells of cajal from the mouse small intestine. Mol Cells 2009;27:525-531.